# **Experimental Studies of Rock Socketed Piles with Different Transverse Reinforcement Ratios**

Rabie Farrag<sup>1</sup>; Benjamin Turner, Ph.D., G.E., P.E.<sup>2</sup>; Carter Cox, P.E.<sup>3</sup>; and Anne Lemnitzer, Ph.D.<sup>4</sup>

## **ABSTRACT**

Piles socketed into rock are frequently utilized to carry large loads from long-span bridges and high-rise buildings into solid ground. The pile design is derived from internal shear and moment magnitudes following code recommendation and numerical predictions. Little experimental data exist to validate code prescriptions and design assumptions for piles embedded in rock. To help alleviate the lack of large-scale test data, the lateral response behavior of three 18-in. diameter, 16 ft long, reinforced concrete piles was evaluated. The pile specimens were embedded in a layer of loose sand and fixed in "rock-sockets," simulated through high strength concrete. The construction sequence simulated soil-pile interface stress conditions of drilled shafts. The pile reinforcement varied to satisfy the internal reaction forces per (1) code requirements, (2) analytical SSI predictions, and (3) structural demands only. The pile specimens were tested to complete structural failure and excavated thereafter. Internal instrumentation along with crack patterns suggested a combined shear-flexural failure, but do not support the theoretically predicted amplification and de-amplification of shear and moment forces at the boundary, respectively.

#### INTRODUCTION

Rock socketed, bored piles are frequently used to transmit large lateral forces to the ground in cases where the soil overlying the rock layer is not capable of providing adequate lateral restraint. Lateral design of rock socketed drilled shafts is commonly based on the beam on an elastic foundation concept (*p-y* curve). Unfortunately, and primarily due to the expensive costs associated with large scale testing, laterally loaded rock-socketed piles have been given limited experimental attention, resulting in a lack of empirical validation of analysis and design methods. Previous experimental research predominantly focused on geotechnical response aspects of rock-socketed piles and the derivation of *p-y* relationships for rock materials (e.g., Frantzen and Stratten, 1987, Carter and Kulhawy, 1992, Dykeman and Valsangkar, 1996, Gabr *et al.*, 2002, Parsons *et al.*, 2010 and Guo and Lehane, 2016).

Impedance contrasts between strong rock layers and softer surface soils have historically challenged design engineers in adequately capturing the internal pile response behavior. Particularly, predictions using Winkler-type foundation analyses yield abrupt changes in the pile's moment profiles which translate into amplified shear forces at the interface boundaries of stiff and soft soil layers. This amplification originates from the differentiation of the fourth order differential beam equation. The foundation engineering community has experienced much

<sup>&</sup>lt;sup>1</sup>Dept. of Civil and Environmental Engineering, Univ. of California, Irvine, CA. Email: irabie@uci.edu

<sup>&</sup>lt;sup>2</sup>Dan Brown and Associates, San Luis Obispo, CA. Email: bturner@dba.world

<sup>&</sup>lt;sup>3</sup>Independent Consultant, Irvine, CA. Email: carterjcox@yahoo.com

<sup>&</sup>lt;sup>4</sup>Dept. of Civil and Environmental Engineering, Univ. of California, Irvine, CA. Email: alemnitz@uci.edu

controversy over whether the large resulting shear demands are representative of actual force effects that must be designed for, or if amplified shear forces are artifacts of the Winkler-type analysis methodology (Caltrans, 2015).

This amplification behavior is not unique to rock-soil interfaces but accompanies many deep foundation elements that cross soil layers with substantially different stiffnesses, or when head or tip restraints control the lateral pile bending behavior. However, the correct evaluation of shear demands at soil-rock socket interfaces is vital since the shear demand may govern the drilled shaft's structural design and the overall constructability of the foundation system. One of the most commonly encountered adverse effects of increased demands in transverse reinforcement is the constriction of concrete flow and the formation of air pockets. Numerical research has attempted to provide insight into the principal mechanism (e.g., Arduino *et al.*, 2018), but no conclusive recommendations are available that can provide sufficient fundamental understanding or data validation to provide informed and reliable design recommendations.

#### **EXPERIMENTAL STUDIES**

The experimental program was executed at the Structural Engineering Testing Hall of the University of California, Irvine. The university has a large reinforced concrete (RC) testbed, casually referred to as "the soil pit" that consists of a strong floor and surrounding concrete walls that serve as reaction elements while lateral load is applied to the pile head. The testbed has a length of 30 ft [9.1 m], a width of 20 ft [6.0 m] width, and a height of 14 ft [4.3 m].

For design purposes, the three rock-socketed test piles were initially modeled and predesigned with LPile (Ensoft, 2018), a commonly used program for analysis of laterally loaded piles. All pile specimens had the same overall geometry, namely (45.7 cm [18 in] in diameter and 477.5 cm [188 in] in total length. The piles were embedded in 1.20 m [4.0 ft] of "rock", simulated experimentally through high strength concrete ( $f_c'$ = 48.3 MPa [7 ksi]). The concrete blocks (i.e., the "rock sockets") had dimensions of 1.83 m [6.0 ft] in length, 1.22 m [4.0 ft] in width, and 1.22 m [4.0 ft] in height. The blocks were secured to the reinforced concrete floor of the testing facility using pre-drilled, epoxy grouted, high strength steel anchors. The piles extended a total of 3.35 m [11.0 ft] outside the rock. The sand overlaying the rock-socket had a thickness of 183 cm [72 in]. A pile cap with cross-sectional dimensions of 0.61 m square [24 x 24 in] and a height of 0.41m [16 in] was constructed on each pile head and used for actuator attachment and application of lateral loading.

All pile specimens had identical longitudinal reinforcement (8 #6 bars, with a ratio of 1.41%), and varied only in transverse reinforcement (Table 1). The transverse reinforcement for Specimen 1 was designed to satisfy the maximum rock socket shear predicted using LPile. Specimen 2 was reinforced with the code-minimum volumetric transverse reinforcement ratio (to satisfy AASHTO LRFD Bridge Design Specs., 8<sup>th</sup> Ed.). And the transverse reinforcement for Specimen 3 was designed so that the nominal shear resistance is equal to the maximum applied shear at the pile head, which results in hoop spacing that exceeds the maximum permissible spacing allowed by codes. The latter configuration is not permitted in any structural design and served for experimental demonstration purposes only. The pile configuration and reinforcement are illustrated in Figure 1.

For an applied lateral pile head load of 58 kN [13 kips], the LPile analysis predicted an amplified pile shear force of 463 kN [104 kips] in the rock socket. This predicted amplified shear corresponds to 8 times the applied lateral head load and more than double the nominal shear resistance provided in Specimen 3 (Figure 2). The stratigraphy and test geometry were chosen to

intentionally exaggerate the shear amplification effect, and to experimentally discern any distinctive failure mechanisms between the three pile specimens.

Table 1. Specimen Design

	Specimen 1	Specimen 2	Specimen 3
Designed to satisfy:	Amplified shear	Code minimum	Applied shear
Transv. reinforcement, bar # @	Spiral #4 @ 114	Spiral #4 @ 152	Ties #3 @ 305
pitch	mm [4.5 in]	mm [6 in]	mm [12 in]
Transv. volumetric reinf. ratio, $\rho_s$	1.27%	0.95%	0.26%
Nominal shear resistance $V_n$	477 kN [107 kip]	396 kN [89 kip]	222 kN [50 kip]
Predicted failure mode based on <i>p</i> -y analysis	Flexural failure	Shear failure	
Predicted pile head load at failure based on <i>p-y</i> analysis	58 kN [13 kip]	52 kN [11.6 kip]	35 kN [7.8 kip]

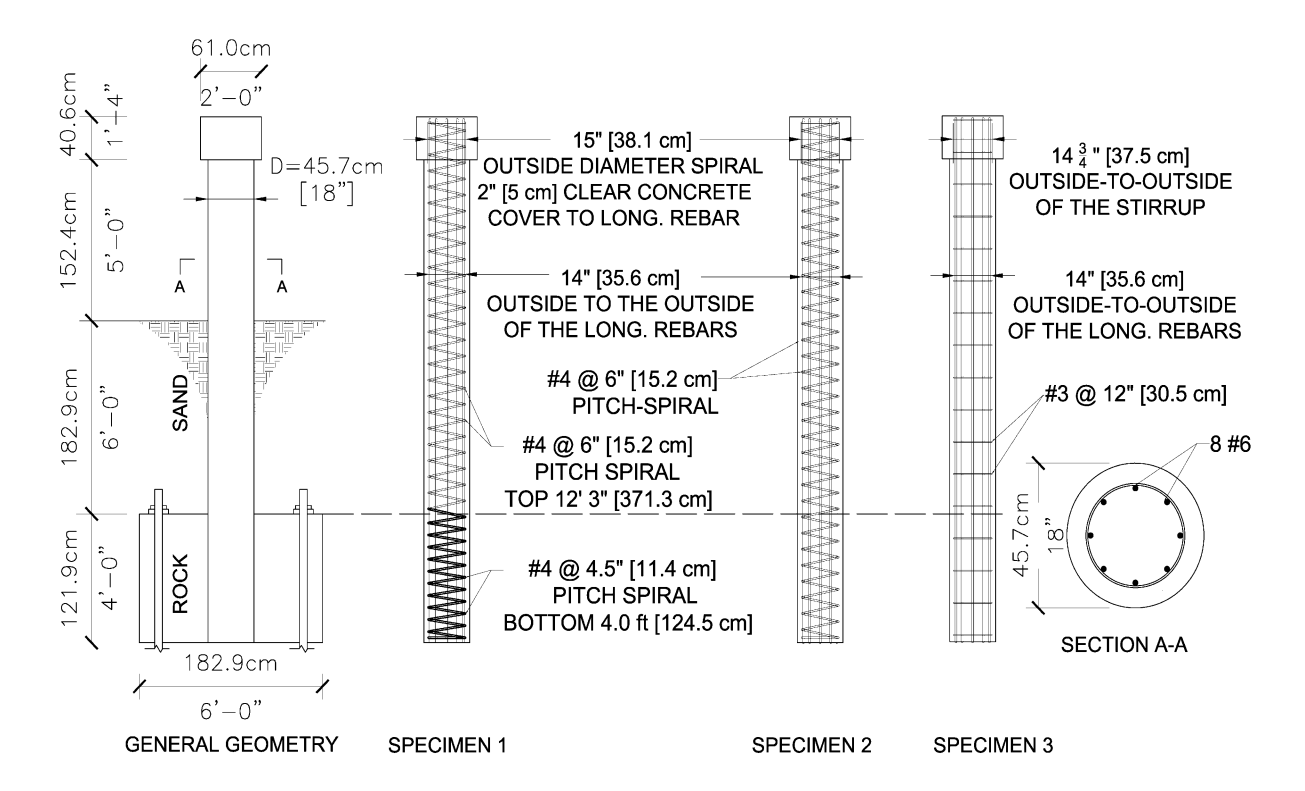


Figure 1. Schematic specimen configuration and variation of transverse reinforcement for all specimens

The specimen instrumentation consisted of internal and external sensors, such as inclinometers, linear voltage differential transducers (LVDTs), strain gauges in longitudinal, rosette, tetrahedral configurations, and string potentiometers. A schematic instrumentation plan for Specimen 1 is exemplarily shown in Figure 3.

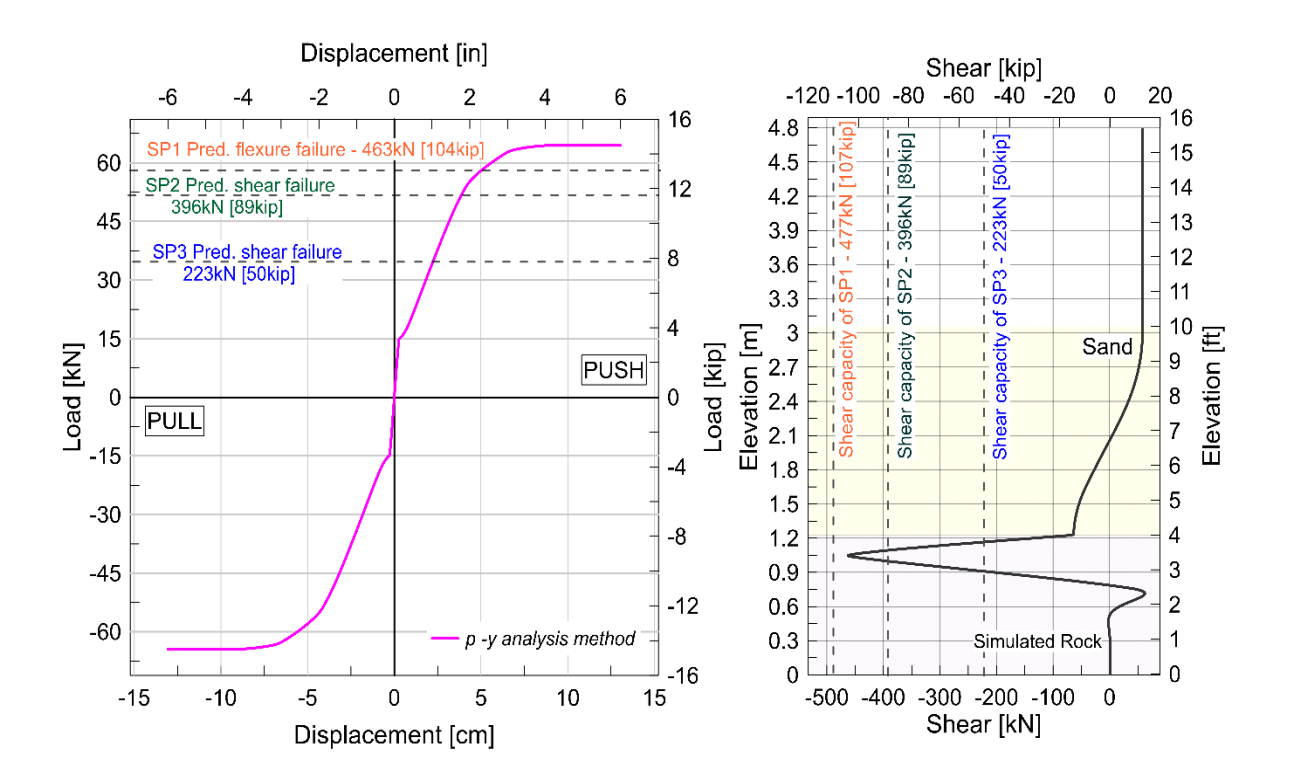


Figure 2. Prediction of pile load-displacement (left) and pile shear forces due to lateral loads 58 kN (13 kips) at the pile head (right).

Figures 4-6 illustrated the construction sequence of the test specimens inside the soil pit. The sand was placed in the pit by dry pluviation using a self-designed and calibrated sieve system attached at the bottom of a concrete hopper, then leveled upon reaching the design height. The intent was to create a relatively loose sand deposit so as to maximize the force effects that reached the rock socket to exaggerate the stiffness contrast between the rock socket and overburden soil. The calibration process included the iteration of adequate fall heights as well as the assembly of multiple sieve openings until the desired relative density was reached. The relatively low in-situ density of 20% provided a strong impedance contrast between the soil and rock materials. Additional in-situ testing of the soil material via cone penetration (CPT) and dilatometer testing (DMT) were used to estimate the soils E-modulus and shear wave velocity; test results are omitted for brevity. The in-situ moisture content of the soil was 6%. The fill sand had a friction angle of 35 deg and cohesion of 5.0 kN/m2 [100 psf], determined through direct shear testing (per ASTM D3080). The average in situ density and relative density were 14.6 kN/m³ [93 pcf] and 20%, respectively.

The rock-socket concrete had a design strength of 34.5 MPa [5ksi], and an average in-situ strength of 48.3 MPa [7ksi] at the day of testing. Pile Specimens 1, 2 and 3 had a design strength of 27.58 N/mm² [4ksi], and an in-situ compressive strength of 40.7 MPa [5.9ksi], 39.3 MPa [5.7ksi], and 39.3 MPa [5.7ksi] at the day of testing, respectively. Compression tests of the rock socket concrete suggested an E-modulus  $E_{\rm conc}$  of 25.5 GPa [3695 ksi]. The soil's E-modulus was derived from DMT testing was found to be around 1.83 MPa[0.261ksi]. The ratio of rock to soil stiffness is  $E_{\rm rock}/E_{\rm soil} = 13,921$ .

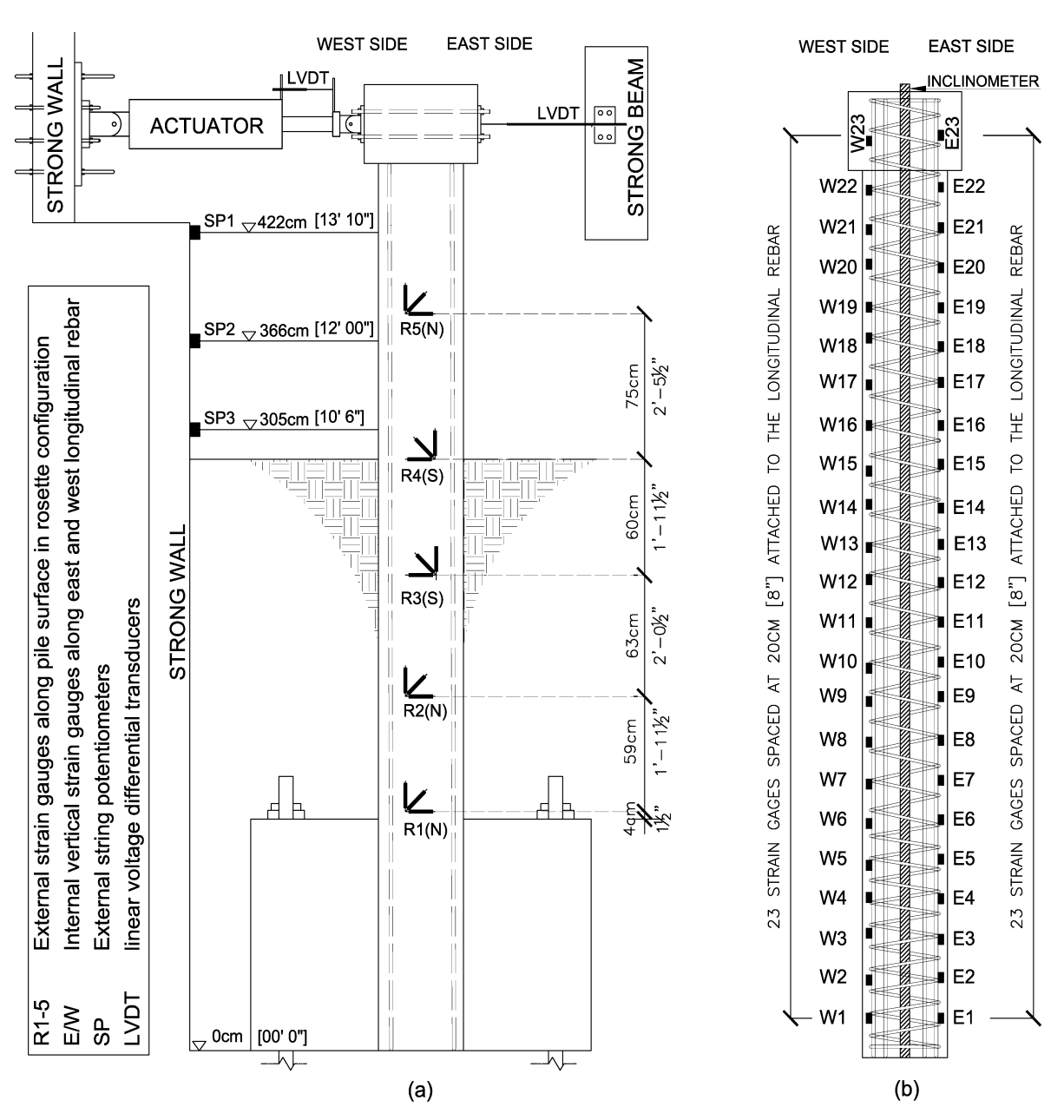


Figure 3. Instrumentation layout for Specimen 1, external sensors (a), and internal sensors (b) (tetrahedral sensors not shown)

The loading protocol was developed based on the predictive analyses shown in Figure 2 and followed the general guidelines of ASCE 41-06, in which applied displacement levels are selected as fractions or multipliers of the anticipated yield displacement. Quasi-static, reverse-cyclic loading was applied at the pile head using three cycles per displacement level up to ultimate capacity. Hereafter two cycles per displacement level were performed until substantial degradation of the load-displacement relationship was noticeable. Loading was applied under displacement control at the center of the pile cap using a 76.2 cm [30 in] stroke, 667 kN [150 kips] capacity hydraulic actuator (see Figures 4 and 6). The pile head displacement history is shown in Figure 7.





Figure 4. Rebar Cages for the three Specimen (left), Installation of Sonotube Formwork around rebar cages (right).





Figure 5. Concrete pour for all three rock-socketed specimens, plus one extra pile (not described in this paper), Pile placement in rock-socket formwork right before concrete placement (right)

The strong wall of the UCI laboratory served as reaction wall. The actuator was controlled by an MTS 407 dual channel controller and data were recorded using a National Instrument data acquisition system. A total of 115 channels were utilized for each test. An externally installed

LVDT, mounted between an independent reference frame and the backside of the pile cap was used to control the experiment and record the pile head displacement.





Figure 6. Completed test setup with pluviated soil prior to testing SP1 (left), Test setup and soil deformation during test of SP3 at 6" lateral displacement (right)

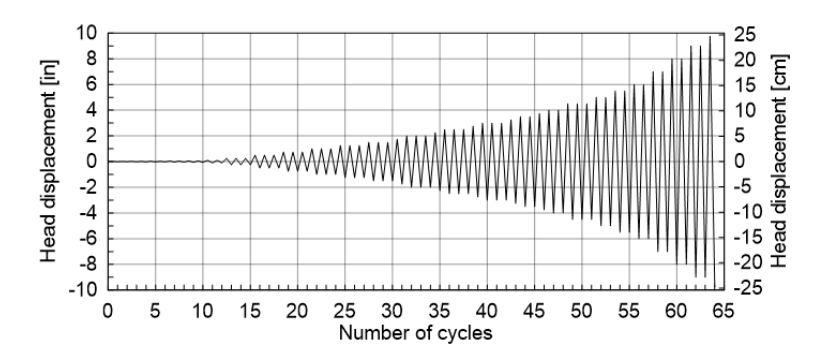


Figure 7. Pile head displacement history and loading cycles for SP1

# **TEST RESULTS**

Figure 8 shows the experimental load displacement behavior of all specimens with their respective backbone curves. Specimen 1 reached an ultimate load of approximately 72 kN [16.2 kips] at a corresponding pile head displacement of 17.8 cm [7.0 in] in push direction, and approximately 72 kN [16.2 kips] at a corresponding pile head displacement of 20.0 cm [7.8 in] in the pull direction. Similarly, Specimen 2 reached ultimate resistance at 71 kN [16 kips] and 17.8 cm [7.0 in] in push direction, and approximately 79 kN [17.8 kips] at a corresponding pile head displacement of 17.8 cm [7.0 in] in pull direction. Specimen 3 reached an ultimate capacity of 77 kN [17.3 kips] at 20.0 cm [7.8 in] of lateral displacement in pull direction and almost similar load levels in push direction.

All specimens behaved identically up to "concrete cracking", i.e., up to a displacement level of 0.64 cm [0.25 in] and a corresponding load of 13.34 kN [3 kips] (about 20% of the ultimate load). The yield displacement was approximately 6.35 cm [2.5 in] at a corresponding load of 8 kips (about 50% of the ultimate load) after which the piles accumulated substantial permanent deformations for repeated loading cycles. Figure 8 also includes a comparison between the

experimental and predicted load displacement curves as well as the predicted failure load levels in flexure (SP1) and shear (SP2 and SP3). The experimental data show that the predicted failure loads have been exceeded by 23%, 53%, and over 100% for SP1, SP2, and SP3 respectively.

The almost identical specimen behavior suggests flexural dominated failure modes for all pile specimens. Specifically, the predicted shear failure due to potential shear amplification near the rock-socket interface would have caused an early failure of SP 2 and SP3 at approximately 52 kN [11 kips] and 35 kN [7.8 kips], respectively, which was not observed experimentally. Instead the pile specimen SP2 and SP3, which were insufficiently reinforced for a potential shear amplification, performed identically to the pile (SP1) which was sufficiently reinforced for the shear amplification and resisted a lateral load of more than 1.6 times the predicted failure limit state.

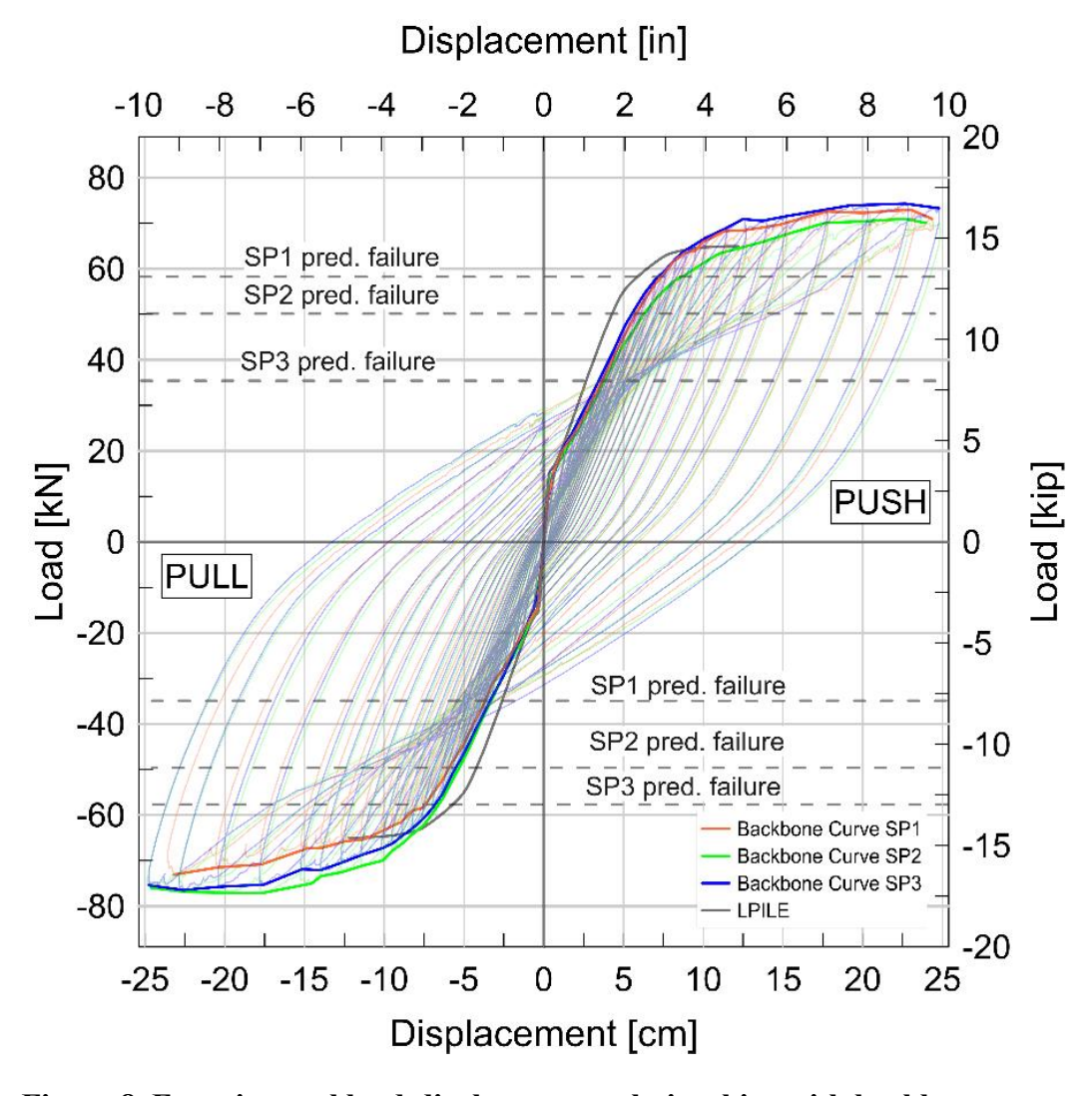


Figure 8. Experimental load-displacement relationships with backbone curve

Figure 9 shows the lateral deformation profiles recorded through the inclinometer instrumentation. Measurements indicate that no deformation occurred within the rock socket. Small lateral pile deformations are noticeable beyond 15 cm [0.5 ft] above the rock socket.

Deformed shapes were similar for all specimens and in both, "pull and push" directions. Curvature profiles [not depicted for brevity] suggest the formation of a plastic hinge within 60 cm [2 ft] above the rock-socket which corresponds to 1.2 m [4 ft] below the ground surface (i.e., about 3 pile diameters (3D)) and agrees well with crack patterns observed upon excavation.

Following test completion, each pile was manually excavated (in push direction) to identify cracking patterns and the location of the plastic hinge. The most substantial cracking concentrated within 61 cm [24 inch] above the rock socket but extended to higher elevations with larger spacings. Almost all cracks formed perpendicular to the pile axis; very few diagonal cracks were recorded. There was no sign of cracking or damage along the socket surface or within the rock socket itself.

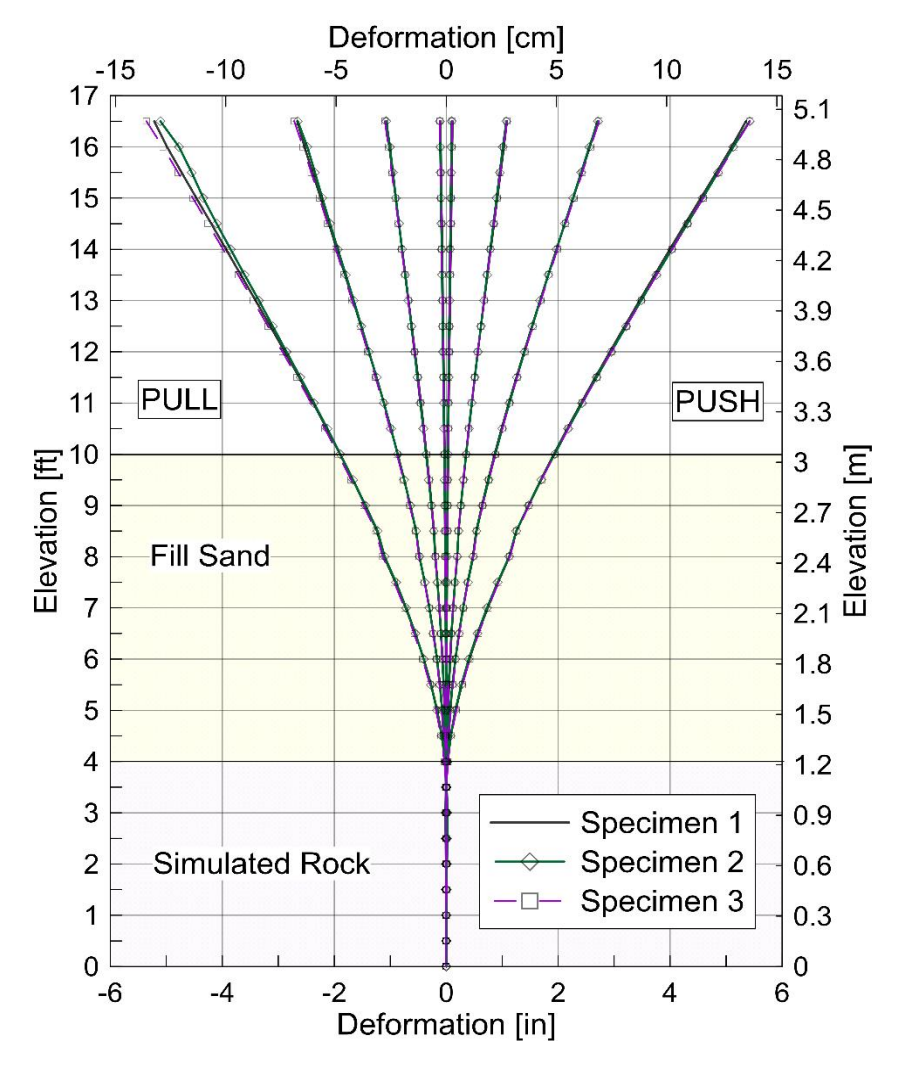


Figure 9. Inclinometer profiles for Specimen 1, 2, and 3 at selected lateral pile head displacement levels (inclinometer readings)

# **SUMMARY**

Three pile specimens with different transverse shear reinforcement were examined under identical test conditions and subjected to reverse cyclic lateral loading. The specimens were

installed in a two-layer soil system with a strong stiffness contrast, namely a loose, silty sand underlain by rock, experimentally simulated through high-strength concrete. Specimens were tested to complete structural failure and excavated after test completion. Despite the significant differences in transverse reinforcement detailing, all three of the piles were interpreted to have failed in flexure without any indication of shear failure – or for that matter, any signs of adverse shear performance – within the rock socket. This is a significant result in light of the fact that pile Specimens 2 and 3 were intentionally designed to reach shear failure prior to flexural failure on the basis of the p-y analyses performed in LPile. For example, recall that the nominal shear resistance of Specimen 3 (222 kN/50 kips) is less than half the predicted amplified shear of 463 kN [104 kips]. This finding confirms the researchers' hypotheses that several factors lead to better-than-expected performance of real rock sockets in comparison to p-y including (1) confinement provided by the rock socket, (2) the fact that a shear failure within the rock socket is kinematically impossible unless accompanied by failure of the surrounding rock mass, and (3) the one-dimensional "beam shear" predicted by the p-y method simply does not capture the actual magnitude and spatial distribution of stresses within the pile and interaction between the pile and rock socket at the concrete-rock interface.

The authors are currently conducting numerical 2D and 3D finite element studies to generate a calibrated model usable for parametric investigations. Unfortunately, results are not available for inclusion in this paper, but will be completed by the time of the conference and presented as part of the results. Numerical studies will provide a closer look at the stress distribution near the rock socket interface, and explore the influence of various rocks strengths as well as soil-rock-stiffness contrasts. The variation of soil-to-rock stiffness contrasts as well as the same phenomenon among soil layers with variable stiffnesses will also be part of the parametric investigations.

## **ACKNOWLEDGEMENTS**

The experimental work was primarily funded through fourth author's NSF funding (CMMI 1752303) along with financial contributions through DFI's Committee project fund, as well as generous industry support from our colleagues at DFI and ADSC. We would like to gratefully acknowledge the leadership and the members of the DFI Drilled Shaft Committee, many of whom provided continuous feedback and guidance during the design and construction process (specifically, Peter Faust, Eric Loehr, and Armin Stuedlein). We are furthermore extremely grateful for the material and equipment donations as well as the engineering support by: PJ Rebar (Nathan King), Atlas Geofoam (Chris Franks), Williams Form Engineering (Pete Speier and Jeff Ohlsen), Foundation Technologies, Inc. (Nick Milligan) and Gregg Drilling and Testing (Brian Savela). Without the support of these colleagues this research program would not have been possible in the scope described.

#### REFERENCES

American Association of State Highway and Transportation Officials, AASHTO. (2017) AASHTO LRFD 8th Bridge Design Specifications. Washington, D.C.

American Concrete Institute. 2019. Building Code Requirements for Structural Concrete (ACI 318-19) and Commentary (ACI 318R-19).

Arduino, P., Chen, L., and McGann, C. (2018). "Estimation of Shear Demands on Rock Socketed Drilled Shafts subjected to Lateral Loading", PEER Report, retrieved from https://peer.berkeley.edu/sites/default/files/2018\_06\_arduino\_final.pdf.

- Brown, D. A., Turner, J. P., Castelli, R. J., and Americas, P. B. (2010). Drilled shafts: Construction procedures and LRFD design methods (No. FHWA-NHI-10-016). United States. Federal Highway Administration.
- Caltrans, F. (2015). *Bridge design practice*, 4<sup>th</sup> edition. California Department of Transportation, Sacramento, CA.
- Carter, J. P., and Kulhawy, F. H. (1992). "Analysis of laterally loaded shafts in rock". *ASCE Journal of Geotechnical Engineering*, Vol. 118, No. 6, pp.270ff.
- Dykeman, P., and Valsangkar, A. J. (1996). "Model studies of socketed caissons in soft rock". *Canadian Geotechnical Journal* 33: 747-759.
- Ensoft, Inc. (2018) LPILE User's Manual. A Program to Analyze Deep Foundations Under Lateral Loading. Austin, Texas.
- Frantzen, J., and Stratten, F. W. (1987). P-y curve data for laterally loaded piles in shale and sandstone. Report No. FHWA-KS-82-2.
- Gabr, M., Borden, R., Cho, K., Clark, S., and Nixon, J. (2002). "P-y Curves for Laterally Loaded Drilled Shafts Embedded in Weathered Rock", Technical Report, North Carolina Department of Transportation, Raleigh, North Carolina.
- Guo, F., and Lehane, B. M. (2016). "Lateral response of piles in weak calcareous sandstone". *Can. Geotech. Journal*, 53: 1424–1434 (2016)
- O'Neill, M. W., and Murchison, J. M. (1983). An evaluation of py relationships in sands. A Report to American Petroleum Institute, PRAC 82-41-1. University of Houston.
- Parsons, R. L., Willems, I., Pierson, M. C., and Han, J. (2010). "Lateral capacity of rock sockets in limestone under cyclic and repeated loading" Report No. K-Tran: KU-09-06.
- Reese, L. (1997). "Analysis of laterally loaded piles in weak rock". ASCE Journal of Geotechnical and Geoenvironmental Engineering, Vol. 123, No. 11.